2009 IEEE International Conference on Control and Automation
Christchurch, New Zealand, December 9-11, 2009

Robust flatness-based control of an AGV under varying load and friction conditions

J. Villagra, D. Herrero-Pérez and M. Abderrahim

Abstract— **This paper presents the control strategy adopted to ensure low jerk variations in path tracking operations of Automated Guided Vehicles (AGVs) in industrial environments. The system is focused on robustness, performance and ease configuration of the maneuvers. Robustness is improved by combining algebraic techniques for robust intelligent feedback control with differential flatness. Besides, it is easily configurable by the definition of a velocity profile decoupled of geometric path. Some simulated results show the dramatic improvement with respect to more standard flatness-based controllers.**

I. Introduction

A. AGVs in industrial environments

The main guidance system in early industrial Automated Guided Vehicles (AGVs) was a wire buried in the floor. A frequency was induced through the wire thus that the AGV could detect and follow it, and thus be directed through its route. In this case, the AGV acts as a kind of dumb-device. The next generation of AGV systems, impelled by the advances and costs reduction in microelectronics and microcomputers, made the AGVs more intelligent, and thus they could make decisions and take part in traffic control of the global system. Besides, new wireless guidance system, using lasers or inertial systems, made the installation of such systems easier.

Wireless guidance systems usually consist of a global positioning system (GPS) to locate the vehicle and a tracking technique to follow a path, which calculates the required control actions. In our case, the AGV, shown in Fig. 1, is a platform of tricycle type and is equipped with a SICK NAV 200 laser navigation system, which provides the location in the environment (GPS). Thus, actions to guide the vehicle are wheel speed and steering angle at each time step.

In order to perform the typical transportation tasks between pickup/delivery (P/D) stations, AGVs should navigate between stations and also achieve precise pickup operations. Navigation between two stations is referred as point-to-point navigation, Fig. 1(a), while precise maneuvers as docking/undocking operations, Fig. 1(b). This work is focused in docking/undocking operations, which should satisfy robustness because slight errors can damage the load or the station. Moreover, the velocity of the AGV, or the time to perform the task, should be as fast as possible. Furthermore, high jerk variations induce vibrations, which could result critic both for the accuracy of the docking/undocking operation and for the stability of the load. Therefore, it is quite interesting that the velocity profile can be configured.

J. Villagra and D. Herrero-Pérez and M. Abderrahim are with the Dept. of Systems Engineering and Automation, University Carlos III, Leganes (Madrid), Spain, jvillagr,dherrero@ing.uc3m.es

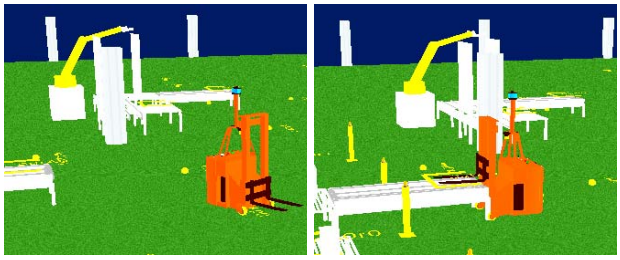

(a) (b)

Fig. 1. (a) AGV navigating (point-to-point) and (b) docking.

This work aims to developed a path tracking technique that reduces jerk variations, and thereby it also reduces the effects of vibrations in the control of AGV and the load. Logically, the tracking method should satisfy a high degree of robustness given the kind of application. Facilities in the configuration of the tracker are also a key point, given that complex set of parameters are usually rather intuitive for operators, instead of, a maximum velocity of operation that satisfies the robustness needed is quite intuitive for them.

B. Control strategies for wheeled mobile robots

Even though wheeled mobile robots control problems have been intensively studied in recent years (cf. e.g. [4] and the references therein), most existing works assume, on the one hand, that they satisfy non-slipping and non-skidding conditions, and on the other hand, that high sample rate measurements are available. However, these assumptions are hardly ever fulfilled, and therefore stability domains and control performance can be significantly altered.

In order to compensate the effects induced by this parameter uncertainty and/or neglected dynamics, several solutions have been proposed. Thus, neural networks [11], fuzzy logic [7], screw theory based control [28], adaptive control ([10], [16], [19]), singular perturbations [2], sliding mode control ([9], [6]) or Lyapunov-based control [1] have been used to address this problem. Most of this approaches need to have a good knowledge of the unmodeled dynamics, or suffer from robustness to demanding disturbances (which are arbitrarily constrained to no nonrealistic bounds).

Besides, an important issue in the nonlinear control of AGVs is that not only a good path tracking has to be assured, but also a good behavior in terms of jerk is desirable. The latter is concerned with the ability to safely dock, undock

978-1-4244-4707-7/09/$25.00 ©2009 IEEE

and carry the pallets, and consequently, with the amount of pallets that can be transported in a single trip.

The best way to achieve both goals is to solve the path-following problem into two subproblems:

- Geometric task, which intends to drive the vehicle as close as possible to the reference path.
- Dynamic assignment task, which assigns a speed profile to the path

In this respect, flatness-based control (cf. [12]) turns out to be a very interesting tool[1] for two main reasons. First of all, because it allows to take advantage of wheeled mobile robots flat structure to simply generate open-loop control to follow the path. Secondly, because a feedback control can be naturally introduced so that time dependence (and therefore the speed profile) is decoupled from the geometric task.

Despite the fact this approach is based only in robot kinematics, its decoupling structure is worth to be preserved. To the best of our knowledge, only [8] has coupled flatness-based control with robust control techniques (sliding modes, to be specific). However, these methods can be constrained by implementation and mechanical issues due to highly switching control actions. Thus, the main contribution of our work is to enlarge robustness properties of the approach introduced by [24] with a control strategy that guarantees low jerk variations.

A final consideration to be taken into consideration for the controller design is that AGV path-tracking maneuvers are presumed to be done in industrial indoor environments with low-cost measurement units. Thus, only GPS and odometry data will be provided to close the control loop. Moreover, the resultant information fusion will be available with very low sample rates. Very few works take into account such kind of limitations, and when they are explicitly treated [17], supplementary sensors are considered. All this challenging conditions will be used in simulations to show the controller performance.

C. Outline of the paper

Section II will be devoted to detail, firstly, how a pure kinematic model is built to represent AGV behavior under ideal circumstances, and secondly, how slipping and skidding effects can naturally be added to the previous model. It will be also shown how load and friction variations can be explicitly introduced in the latter model. Flatness-based control will be recalled in section III, where the kinematic model will be used to obtain an open-loop control (section III-A). A first feedback control strategy will be presented in section III-B, for which a reference path and a speed profile have to be analytically computed (section III-C). Since the resulting control presents poor robustness properties under severe skidding and slipping disturbances, a MIMO intelligent feedback control has been introduced (section IV). Section V will show the dramatic improvement with respect to more standard flatness-based controllers through simulation results. Finally, some concluding remarks and future work will be provided (section VI).

[1]Some authors proposed alternative techniques (cf. i.e. [1]) to solve this problem, but they generally result in more conservative results.

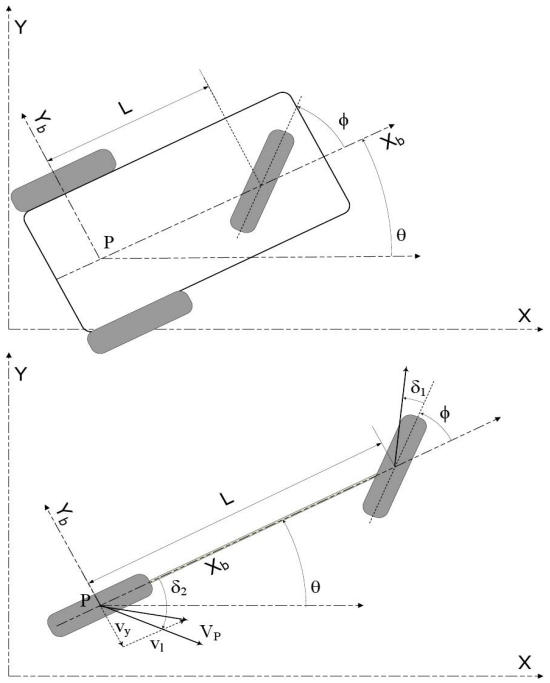

Fig. 2. (a) Purely kinematic wheeled mobile robot and (b) skidding and slipping wheeled mobile robot.

II. Wheeled mobile robot model: from kinematics towards skidding and slipping

A. Pure kinematic model

The wheeled mobile robot considered in this paper has a body frame X_b, Y_b attached to the reference point P with coordinates $\xi = (x,y)^T$ in global coordinate frame $\{X,Y\}$ as shown in Fig. 2(a). θ denotes the orientation of the basis $\{X_b, Y_b\}$ with respect to the global frame, so that the generalized coordinates of this wheeled mobile robot are $q = (x,y,\theta)$. The robot is equipped with a front-centered steerable wheel (whose angle is represented by ϕ) and fixed parallel rear wheels.

The system is subject to two nonholonomic constraints, one for front wheel, and another for rear wheel:

$$\begin{aligned} \dot{x}_f \sin(\theta+\phi) - \dot{y}_f \cos(\theta+\phi) = 0 \\ \dot{x}_f \sin(\theta) - \dot{y}_f \cos(\theta) = 0 \end{aligned} \tag{1}$$

where $x_f = x + L\cos\theta$ and $y_f = y + L\sin\theta$ denote the cartesian coordinates of the front wheel, and L is the distance between the wheels. If equation (1) is entirely expressed in terms of x and y, the following Pfaffian constraint matrix can be written:

$$C(q) = \begin{bmatrix} \sin(\theta+\phi) & \cos(\theta+\phi) & -L\cos(\phi) \\ \sin(\theta) & -\cos(\theta) & 0 \end{bmatrix} \tag{2}$$

All admissible generalized velocities are contained in the one-dimensional null space of the constraint matrix $C(q)$. In

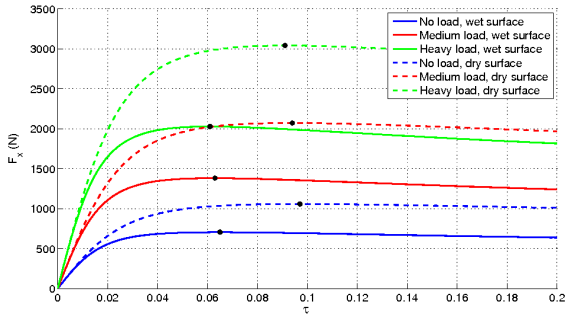

Fig. 3. Maximum longitudinal force F_x in terms of slip ratio τ for several friction μ and load conditions F_z.

other words, the resulting state-space kinematic model will be obtained as a function of the vector defining that kernel basis:

$$\begin{bmatrix} \dot{x} \\ \dot{y} \\ \dot{\theta} \end{bmatrix} = \begin{bmatrix} \cos\theta \\ \sin\theta \\ \frac{v}{L}\tan\phi \end{bmatrix} \tag{3}$$

B. Skidding and slipping model

1) Slipping: Under pure rolling assumption, where there is no tire deformation, the wheel's linear velocity is $v_l = r\omega$. However, this is not the case when an important load or acceleration is applied to the vehicle. The wheel slipping can be characterized by slip ratio $\tau = \frac{r\omega - v_l}{r\omega}$, $\tau \in [-1,1]$. Equivalently, a longitudinal slip velocity can be defined as $d = r\omega - v_l$.

Fig. 3 shows the relationship between longitudinal braking efforts and slip ratios provided by Pacejka tire model[2], from which two main issues may be highlighted:

- Vertical effort F_z, which measures vehicle load, and friction coefficient μ, are related to longitudinal effort with $F_x = \mu F_z$. As a result, it is not difficult to understand that maximum allowable braking (or accelerating) actions are always greater in a dry road ($\mu = 0.9$) and with a heavy load, than in a wet surface ($\mu = 0.6$) with a small load (see black points in Fig. 3, which are obtained using $F_{x_{\max}} = \mu_{\max} F_{z_{\max}}$).
- A linear zone, followed by a nonlinear one, leads systematically to maximum points (black points in Fig. 3) in the F_x-τ plane. An AGV almost always works in the linear zone, except if adherence and load conditions are not taken into account. In that case, wheels saturation may arise when slip ratio is bigger than in the maximum peak.

To sum up, even if a similar pattern exist for every plotted case, a strong dependency on load and friction conditions can be observed. In order to overcome this modeling problem, slip velocity d can be analytically approached[3] in terms of tire slip stiffness K_x, load mass m, longitudinal velocity v_l and acceleration γ_x, by considering $F_x = K_x\tau = m\gamma_x$

$$d = \frac{m\gamma_x}{K_x} v_l \tag{4}$$

This approximation will be used in the wheeled mobile model (eq. 7) to introduce slipping behavior in the linear velocity ($v_l = r\omega - d$).

2) Skidding: When a turning maneuver begins, a cornering force acts laterally on the wheel's contact patch, causing the wheel to transverse along a direction away from the wheel's plane. This behavior is referred to as skidding. The angle between the wheel's direction of travel and the wheel's plane is known as the slip angle δ.

Consider that the fixed parallel wheels can be simplified by a fictitious wheel at the center of those parallel wheels. Denote V_P as the velocity of the reference point P (see Fig. 2); v_y denotes the projection of velocity V_P on the direction of Y_b, and v_l represents the beforehand mentioned linear wheel's velocity, which is the velocity V_P projected on the direction of X_b. These two velocities (v_l, v_y) are related to the slip angle δ by the geometric relationship $\tan\delta = \frac{v_y}{v_l}$.

Fig. 2(b) shows the motion of the robot using a wheeled mobile robot model in the presence of skidding and slipping, where ϕ denotes the robot front steering angle, δ_1 represents the slip angle of the front wheel and δ_2 the generalized slip angle of the rear fictitious wheel.

To derive the non-holonomic constraint equation in the presence of skidding and slipping, we extend the equation formulation used in the ideal cases (1) to the situations with skidding and slipping.

The rear fixed wheel leads to the following constraint equation by projecting velocity V_P along its perpendicular direction:

$$\begin{bmatrix} -\sin\delta_2 & \cos\delta_2 \end{bmatrix} R(\theta)\dot{\xi} = 0 \tag{5}$$

where R is an orthogonal rotation matrix

$$R = \begin{bmatrix} \cos\theta & \sin\theta \\ -\sin\theta & \cos\theta \end{bmatrix}$$

In a similar way, the front steerable wheel introduce the following constraint:

$$\begin{bmatrix} -\sin(\delta_1+\gamma_1) & \cos(\delta_1+\gamma_1) \end{bmatrix} R(\theta)\dot{\xi} + L\cos(\delta_1+\gamma_1)\dot{\theta} = 0 \tag{6}$$

Solving constraints (5) and (6) leads to a kinematic model of the robot which includes sliding and slipping (see [27] for more details):

$$\begin{bmatrix} \dot{x} \\ \dot{y} \\ \dot{\theta} \end{bmatrix} = \begin{bmatrix} v_l\cos\theta - v_y\sin\theta \\ v_l\sin\theta + v_y\cos\theta \\ \frac{v_l}{L}\tan(\gamma_1+\delta_1) - \frac{v_y}{L} \end{bmatrix} \tag{7}$$

[2]The pseudostatic model from [23] gives a good approximation to experimental results and is widely used in automotive research and industries. An overview on tire effort models and its estimation can be found in [25]

[3]This approximation is only valid under a low slip ratio assumption, i.e when $F_x = K_x\tau$, where an off-line identified parameter K_x measures the tire ability to generate longitudinal efforts at low speeds.

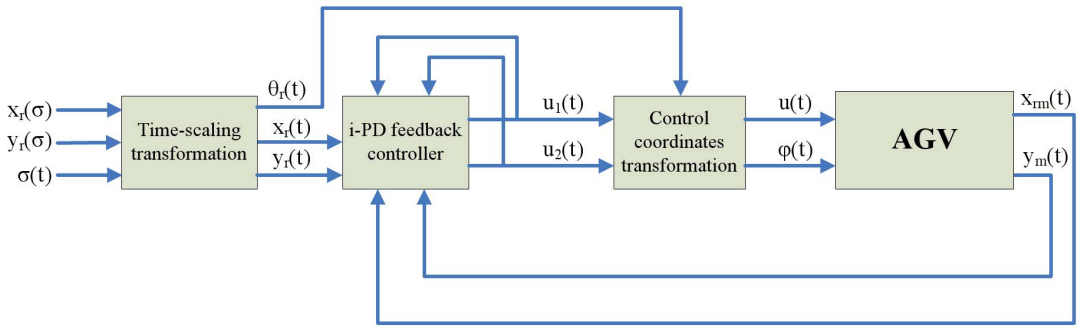

Fig. 4. Scheme of a flatness-based control with intelligent feedback for AGV path tracking.

III. Control strategy

Fig. 4 depicts the control scheme that will be detailed in the following paragraphs. The flat nature of system 3 will be exploited to turn this MIMO nonlinear problem into two decoupled SISO pole-placement problems. To that end, a time-scaling transformation (section III-A), together with a trajectory stabilizing dynamic feedback controller (section III-C), will be applied to the robot. Since this dynamic feedback is loosely equivalent to a control coordinates transformation, a final block will reconvert fictitious control variables to real ones (section III-B). Finally, in order to guarantee a high degree of robustness to load and friction variations, an intelligent PD controller will complement the initial feedback controller (section IV).

A. Flatness-based control

Broadly speaking, a dynamic system ($\dot{x} = f(x,u), x \in \mathbb{R}^n, u \in \mathbb{R}^m$) is differentially flat [12] if there exist a set of variables $z \in \mathbb{R}^l$ called flat outputs such that:

1) the components of these flat outputs are variables of the system or can be simply expressed in terms of the system variables.
2) the components of the flat outputs are not related by any differential equation, and therefore, it is possible to plan their trajectories in order to control the system
3) every system variable (including control variables) can be expressed in terms of the flat outputs and its derivatives. As a result, no differential equation integration is needed to obtain the open-loop control of the system.

As shown in [12], the kinematic model of the wheeled mobile robot given in equation (3) is flat with flat outputs[4] $z = \{x, y\}$. The three conditions above enounced to establish the flatness of a system can be verified in our case with the following expressions, which are easily obtained from (3):

$$\theta(t) = \arctan\left(\frac{\dot{y}(t)}{\dot{x}(t)}\right) \tag{8}$$

$$u(t) = \sqrt{\dot{x}^2(t) + \dot{y}^2(t)} \tag{9}$$

$$\phi(t) = \arctan\left(\frac{L\left(\dot{x}(t)\ddot{y}(t) - \ddot{x}(t)\dot{y}(t)\right)}{\left(\dot{x}(t) + \dot{y}(t)\right)^{3/2}}\right) \tag{10}$$

It is important to notice that classical stabilization schemes, such as static feedback linearization, are not suitable for this problem; time-varying (or dynamic) feedback[5] is required here due to unavoidable singularity in the decoupling matrix associated with linearization problem (see [13] for more details).

However, even if dynamic feedback permit to avoid the beforehand mentioned problems, the open-open control proposed in (9) and (10) may exhibit undesirable discontinuities when velocity approaches to zero.

In order to avoid such singularities, [13] introduced a time-scaling tool, which may be interpreted as controlling the clock. But this time-scaling is not only important to obtain a consistent open-loop steering control; it also turns out to be very useful for the design of trajectory stabilizing feedback controllers.

B. A stabilizing feedback controller

Following the dynamical extension algorithm[6], the flat outputs are differentiated until the controls u and ϕ appear. As a result, u and ϕ can be expressed in terms of $\ddot{x}$ and $\ddot{y}$, and therefore, an endogenous dynamic feedback can be written as follows:

$$\begin{aligned} \ddot{x} &= v_1 \\ \ddot{y} &= v_2 \end{aligned} \tag{11}$$

where the fictitious controls v_1 and v_2 are obtained by differentiating equations (3)

[4]One of the most relevant aspects of differential flatness for control engineers is that the flat output often corresponds to a set of real outputs of the system, which have also a physical meaning

[5]Flat systems are equivalent to controllable linear ones via a special type of dynamic feedback called endogenous

[6]The input-output decoupling problem, which consists on finding a feedback such that each output component is affected by one and only one input component, can be solved with the Dynamic Extension Algorithm (see [22]).

$$\begin{bmatrix} v_1(t) \\ v_2(t) \end{bmatrix} = \begin{bmatrix} \cos\theta(t) & -\dfrac{u^2(t)}{L}\sin\theta(t) \\ \sin\theta(t) & \dfrac{u^2(t)}{L}\cos\theta(t) \end{bmatrix} \begin{bmatrix} \dot{u}(t) \\ \tan\phi(t) \end{bmatrix} \tag{12}$$

Using the time scaling procedure previously mentioned, a parameter change $t \mapsto \sigma(t)$ will be applied, with σ an increasing function. Thus, equation (3) will remain unchanged by introducing $\dfrac{d}{dt} = \dot{\sigma}\dfrac{d}{d\sigma}(t)$, except that $u(t)$ will become $u(\sigma(t))\dot{\sigma}$. Since a robust behavior to disturbances or unmodeled dynamics is sought, a stabilizing closed-loop control strategy has to be implemented. In this respect, time scaled feedback linearization turned out to be consistently better than other path tracking approaches (see [3] for an experimental comparison). Thus, error dynamics on x and y has to be exponentially driven to zero as follows

$$\begin{aligned} v_1(t) =& \ddot{x}_r(\sigma(t)) + K_{D1}\left(\dot{x}_r(\sigma(t)) - \dot{x}_e(t)\right) + \\ &+ K_{P1}\left(x_r(\sigma(t)) - x_e(t)\right) \\ v_2(t) =& \ddot{y}_r(\sigma(t)) + K_{D1}\left(\dot{y}_r(\sigma(t)) - \dot{y}_e(t)\right) + \\ &+ K_{P2}\left(y_r(\sigma(t)) - y_e(t)\right) \end{aligned} \tag{13}$$

where estimated position values x_e, y_e and their time derivatives have to be obtained from available measurements.

Remark 3.1: Numerical differentiation and filtering has been already attacked by numerous means and techniques. Any robust and efficient approach could be used here, but the implemented solution is based on a novel powerful tool developed by [20].

Finally, if the time scaling is applied to the inversion of (12), a closed-loop control on steering angle and longitudinal velocity can be written as follows:

$$\begin{aligned} \dot{v}(t) &= \dot{\sigma}\left(\cos\theta_r(\sigma(t))v_1(t) - \sin\theta_r(\sigma(t))v_2(t)\right) \\ u(t) &= v(t)\dot{\sigma}(t) \\ \phi(t) &= \arctan\left(\frac{L}{v(t)^2}\left(\cos\theta_r(\sigma(t))v_2(t) - \right.\right. \\ &\quad \left.\left. - \sin\theta_r(\sigma(t))v_1(t)\right)\right) \end{aligned} \tag{14}$$

Remark 3.2: Remark that, besides x_r and y_r, the third reference generalized coordinate θ_r explicitly appears in equation (14). The flatness property of this system allows to write θ_r in terms of the flat outputs $\{x, y\}$, as shown in equation (8).

To achieve such stabilization, not only admissible reference trajectories [5] have to be off-line computed, but a speed profile has also to be provided.

C. Reference trajectories generation

As explained in the introduction, the proposed control strategy will be used for docking/undocking maneuvers. Thus, a sufficiently smooth geometric path, which takes robot kinematic constraints into account, will be generated before such maneuvers.

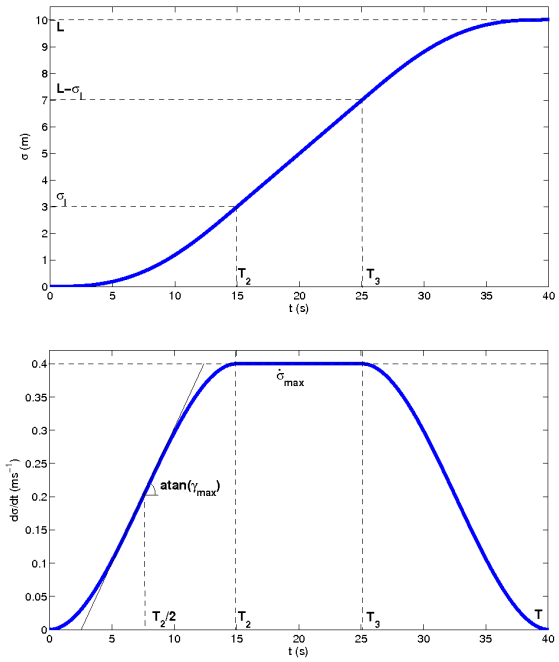

Fig. 5. (a) Arc length and (b) arc length derivative evolution in terms of time.

Besides, arc length $\sigma(t)$ and its derivative $\dot{\sigma}(t)$ have to be provided to achieve the time scaling transformation Since the wheeled mobile robot has velocity and acceleration limitations ($\dot{\sigma}_{max}$ and γ_{max}, respectively), a closed-form arc length profile will be obtained in terms of those two parameters.

Consider an increasing function $\sigma(t)$, whose evolution is depicted in Fig. 5, and parameterized with the following piecewise polynomial function:

$$\sigma(t) = \begin{cases} a_1t^3 + b_1t^2 + c_1t + d_1, & 0 \leqslant t < T_2 \\ a_2t + b_2, & T_2 \leqslant t < T_3 \\ a_3t^4 + b_3t^3 + c_3t^2 + d_3t + e_3, & T_3 \leqslant t \leqslant T \end{cases} \tag{15}$$

with L the total arc length of the docking path, $T_2 = \dfrac{\dot{\sigma}_{max}}{\gamma_{x_{max}}}$, $T = 2T_2 + \dfrac{L - 2\sigma_I}{\dot{\sigma}_{max}}$ and $T_3 = T - T_2$.

Remark that three different zones exist both in $\sigma(t)$ and in $\dot{\sigma}(t)$: an acceleration phase, a constant velocity phase and a decelerating phase. Since the maximum attainable acceleration is precisely obtained at the middle point of the first phase, time parameter T_2 can be directly deduced from $\sigma(t)$ and $\dot{\sigma}(t)$. From that, it is straightforward to obtain the other meaningful instants (T_3 and T).

Polynomial coefficients of (15) are obtained by solving the piecewise linear system that fulfills the following continuity constraints:

$$\begin{aligned} &\sigma(0) = 0,\ \dot{\sigma}(0) = 0,\ \dot{\sigma}(T_2) = \dot{\sigma}_{max},\ \ddot{\sigma}(T_2) = 0 \\ &\sigma(T_3) = L - \sigma_I,\ \sigma(T) = L,\ \dot{\sigma}(T_3) = \dot{\sigma}_{max},\ \dot{\sigma}(T) = 0 \\ &\ddot{\sigma}(T_3) = 0 \end{aligned}$$

where $\sigma_I = \dfrac{2\dot{\sigma}_{max}^2}{3\gamma_{x_{max}}}$.

Remark 3.3: As mentioned, one of the main features of this approach is its ability to decouple geometry from target velocities. Thus, a velocity profile will be automatically generated by specifying only these two parameters.

IV. Intelligent[7] feedback control

The proposed time-scaling endogenous dynamic feedback guarantees a robust stabilization when initial conditions are not well known or soft disturbances are applied to the robot (cf. [3] and [13]). However, the convergence speed and the stability regions are significantly affected when important unmodeled dynamics or disturbances perturb the nominal behavior of the system.

The main contribution of this work is the introduction of intelligent PID (i-PID) controllers to improve the dynamic behavior of the wheeled mobile robot under a high degree of uncertainty.

The main advantage of this approach is that it uses a standard PID controller structure, but it is able to take into account, without any modeling procedure, the unknown parts of the system. It is based on a fast and easily implementable online numerical differentiator (cf. [14] or [15] for further details). These techniques, based on differential algebra (cf. [14]) are also used, as stated in remark 3.1, in equations (13).

Consider a finite-dimensional MIMO system, with m inputs $u = (u_1, \ldots, u_m)$ and n outputs $y = (y_1, \ldots, y_n)$:

$$\Phi_j(y, \ldots, y^{(N_j)}, u, \ldots, u^{(M_j)}) = 0,\ j = 1 \ldots n \tag{16}$$

If the assumption $\dfrac{\partial \Phi_j}{\partial y_j^{(n_j)}} \neq 0,\ j = 1 \ldots n$ is verified, the implicit function theorem and a straightforward simplification (cf. [14]) locally yields

$$\begin{aligned} y_1^{(\mu_1)} &= F_1 + \alpha_{1,1} u_1 + \ldots + \alpha_{1,m} u_m \\ &\ldots \\ y_n^{(\mu_m)} &= F_n + \alpha_{n,1} u_1 + \ldots + \alpha_{n,m} u_m \end{aligned} \tag{17}$$

where $\alpha_{i,j}, i = 1 \ldots n, j = 1 \ldots m$ and $\mu_j, j = 1 \ldots m$ are non-physical constant parameters, which are chosen by the engineer with the following guidelines:

- μ_m will be an integer value (usually 1 or 2), which may represent the system degree, but not necessarily
- $\alpha_{i,j}$ are chosen in such a way that F_j and $\alpha_{i,j} u_j$ are of the same magnitude

Finally, $F_j,\ j = 1 \ldots m$ are determined thanks to the knowledge of u_j, $\alpha_{i,j}$ and of the estimates of $y_j^{(\mu_j)}$

$$F_j(t_k) = [y_j^{(n_j)}(t_k)]_e - \sum_{i=1}^{m} \alpha_{j,i} u_i(t_{k-1}) \tag{18}$$

[7]Remark that this notation is not related to artificial intelligence techniques, but rather to the capacity to automatically complete what a standard linear controller cannot do.

In fact, the F_j terms carry the whole information on the process to be controlled (which might include hardly identifiable parameters or complex time-varying phenomena, like frictions). It is somehow similar to a black-box identification, but without any restriction about the model validity domain.

The endogenous feedback beforehand detailed (eq. (11)) permit to decouple the nonlinear model (2). This fact leads to a specially easy tuning of the MIMO i-PID, because the general model (17) yields for this specific case:

$$\begin{aligned} x^{(\mu_1)}(t) &= F_1(t) + \alpha_1 v_1(t) \\ y^{(\mu_2)}(t) &= F_2(t) + \alpha_2 v_2(t) \end{aligned} \tag{19}$$

where μ_1 and μ_2 can be naturally replaced by 2; $\alpha 1$, $\alpha 2$ can be set to 1, and $F_1(t_k) = x_e^{(2)}(t_k) - v_1(t_{k-1})$, $F_2(t_k) = y_e^{(2)}(t_k) - v_2(t_{k-1})$. Finally, equation (19) will be used to complement (13) in the final i-PD feedback controller block of Fig. 4 as follows

$$\begin{aligned} v_1 &= \ddot{x}_r - F_1 + K_{P_x} e_x + K_{D_x} \dot{e}_x \\ v_2 &= \ddot{y}_r - F_2 + K_{P_y} e_y + K_{D_y} \dot{e}_y \end{aligned} \tag{20}$$

with

- x_r and y_r the reference docking/undocking path.
- $e_x = x - x_r$ and $e_y = y - y_r$ the longitudinal and lateral tracking errors,
- K_{P_x} , K_{D_x} , K_{P_y} and K_{D_y}, suitable PD controller gains.

V. Robustness analysis under friction and load variations

A spline-smoothed path respecting a maximum allowable steering angle $\phi = \pm 60^\circ$ (see Fig. 6) will be used to simulate the AGV behavior in a docking maneuver under different load and friction conditions. A velocity profile as that depicted in fig. 5 will be used to cover the whole path at a maximum speed $\dot{\sigma}_{max} = 0.4$ ms^{-1} and with a maximum acceleration $\gamma_{x_{max}} = 0.05$ ms^{-2}. This profile (see Fig. 7) may seem too conservative, but current AGVs usually operate at similar speeds in docking/undocking maneuvers. Nevertheless, one of the main advantage of the proposed approach is that any maximum velocity and acceleration could have been used to analytically obtain the velocity profile, which will always be independent of the geometric path.

In a first step, the endogenous stabilizing feedback control is applied to a pure kinematic model (3). GPS measurements are available only once per second and wheel angular velocities sampling frequency is constrained by control cycle duration ($T_s = 0.111$s). Both values can be merged in an adaptive filter (an extended Kalman filter or similar), where measurement noises have to be characterized. In all the below simulations, odometry values are supposed to be corrupted with an additive white gaussian noise $\mathcal{N}(0, \varsigma)$ whose standard deviation is $\varsigma = 10^{-3}$.

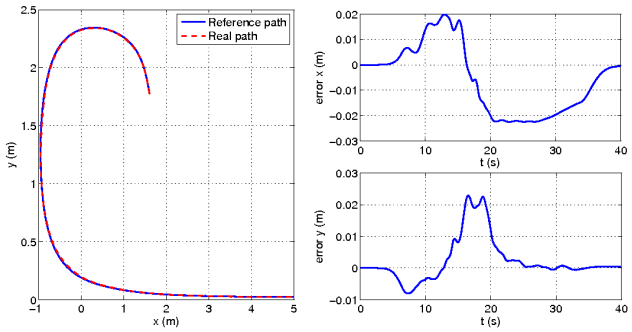

Fig. 6. Reference docking path and real path followed by the vehicle without slipping and skidding effects (left). Tracking errors on x and y coordinates (right).

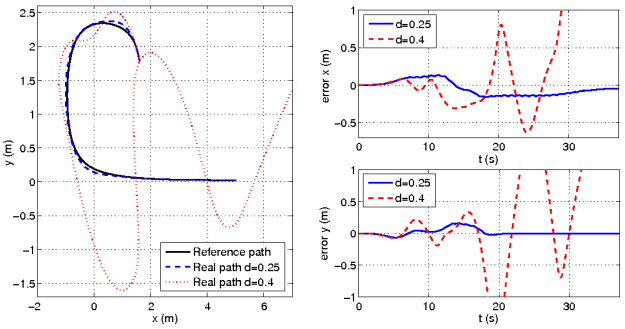

Fig. 8. Standard endogenous feedback control. Reference docking path and real path followed by the vehicle with slipping and skidding effects (left). Tracking errors on x and y coordinates (right).

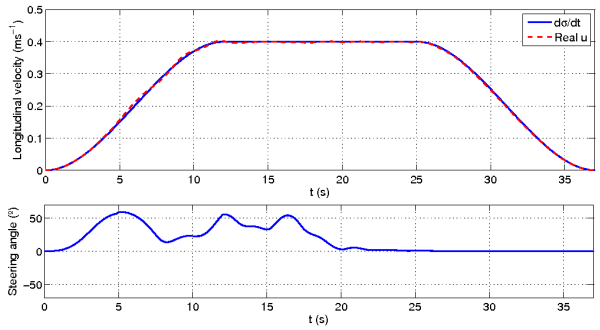

Fig. 7. Longitudinal velocity and steering angle with a pure kinematic wheeled mobile robot. Flatness-based open-loop control with an endogenous stabilizing feedback.

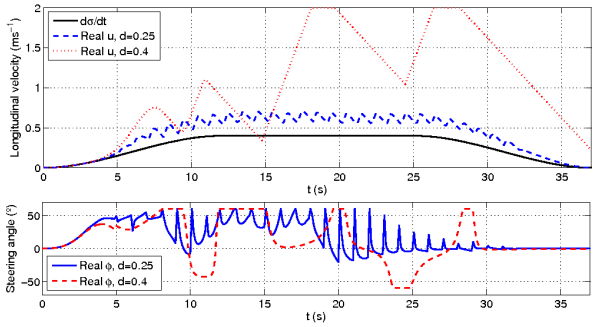

Fig. 9. Longitudinal velocity and steering angle with a skidding and slipping wheeled mobile robot. Flatness-based open-loop control with an endogenous stabilizing feedback.

Fig. 6 shows the tracking performance of the vehicle with all these conditions. It can be observed that error on x and y components are really reduced and tend to completely disappear when approaching to the docking point. The small errors, which come from the low-rate noisy measurements, could be much smaller if no feedback were introduced. However, since control system robustness is under study, feedback will be kept and evaluated under severe disturbances.

Moreover, jerk variations will be also observed in order to estimate the number of pallets which can be safely carried. In Fig. 7, control actions are plotted to give an insight of this sort of "transportability'. Both steering angle and velocity exhibit a very smooth behavior.

Consider now model (7) with skidding and specially slipping effects (or, in other words, with very different load and friction conditions). Lateral velocity v_y will be modelled as the output of a second order linear system whose input is steering angle (see [21] for further details). Very high slip velocities d will be used in order to simulate critical situations, where the maximum accelerating force in the $F_x - \tau$ plane (Fig. 3) is by far exceeded.

Fig. 8 and Fig. 9 permit to see how difficult is to track the desired path when high slip velocities $d = 0.25$ and $d = 0.4$ are considered. In the first case, the final point is attained with a reasonable error. However, the necessary control actions present an inadmissible chattering nature to respect the transportability criteria (Fig. 9). In the second case, the system is out of control because steering angle and velocity saturation constraints are systematically violated.

Finally, figures 8 and 9 show that when the i-PD feedback control is applied to the same benchmark, a remarkable improvement is obtained. Indeed, not only a much better tracking performance, but also much smoother velocity and steering angle controls, are observed in both cases.

It is then clear that the introduction of an auto-adaptive (intelligent) feedback control considerably enhance not only the system robustness and stability domain, but also the smoothness of the robot motion. As a result, a higher pallet stack will can be safely conveyed.

Remark 5.1: Even if this preliminary work only presents simulation results, they show a significant enhancement when compared to more classical flatness-based controllers. Thus, a campaign of experiments on a real AGV platform [18] is currently under development, and the subsequent results will be soon published.

VI. Conclusion and Future Work

Algebraic techniques for robust feedback control have been combined with differential flatness to obtain a control strategy, specially well suited for AGV path tracking in industrial environments. Simulations have shown very interesting results with no need of physical parameters knowledge

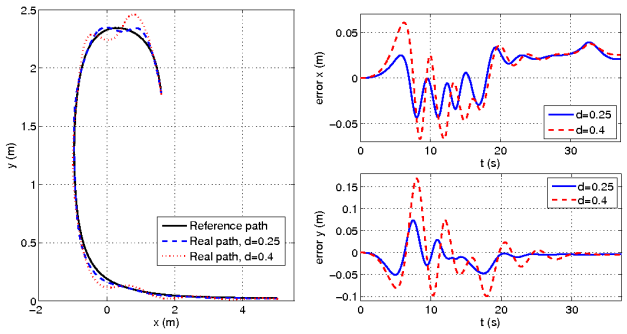

Fig. 10. i-PD flatness-based control. Reference docking path and real path followed by the vehicle with slipping and skidding effects (left). Tracking errors on x and y coordinates (right).

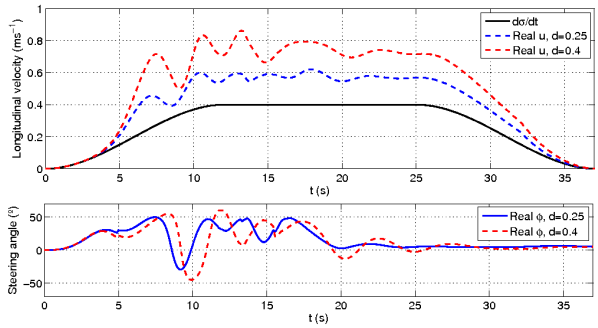

Fig. 11. Longitudinal velocity and steering angle with a skidding and slipping wheeled mobile robot. Flatness-based open-loop control with an i-PD feedback.

and with a high degree of efficiency (performance, computational cost and calibration time).

Experimental results will be soon available to validate the main features highlighted in this paper. Besides, an exhaustive investigation of stability domains and noise influence in filtering techniques will be necessary for a commercial use.

Concerning the latter, a novel method to easily merge GPS and odometry information will be presented in an upcoming work. The closed-loop system behavior using this technique will be compared, in terms of computational cost and performance, with an Extended Kalman based approach.

REFERENCES

[1] A.P. Aguiar, and J.P. Hespanha, 'Trajectory-tracking and path-following of underactuated autonomous vehicles with parametric modeling uncertainty', *IEEE Transactions on Automatic Control*, Vol. 52, No. 8, pp. 1362–1379, 2007.

[2] B. d'Andréa-Novel, G. Campion, and G. Bastin, 'Control of non-holonomic wheeled mobile robots by state feedback linearization', *International Journal of Robotic Research*, Vol. 14, No. 6, pp. 543–559, 1995.

[3] F. Bullo, and R.M. Murray, 'Experimental comparison of trajectory trackers for a car with trailers', *13th IFAC World Conference*, pp. 407–412, San Francisco, 1997.

[4] C.Canudas de Witt, B. Siciliano, and G. Bastin, 'Theory of Robot Control', Springer, UK, 1997.

[5] O. Chocron, E. Deleleau, and J.L. Fleureau, 'Flatness-based control of a mechatronic weed killler autonomous robot, *Proc. of IEEE International Symposium on Industrial Electronics*, pp. 2214–2219, Vigo (Spain), 2007.

[6] M.L. Corradini, T. Leo, and G. Orlanndo, 'Experimental testing of a discrete-time sliding mode controller for trajectory tracking of a wheeled mobile robot in the presence of skidding effects', *Journal of Robotic Systems*, Vol. 19, No. 4, pp. 177–188, 2002.

[7] T. Das, and I.N. Kar, 'Design and implementation of an adaptive fuzzy logic based controller for wheeled mobile robots', *IEEE Transactions on Control Systems Technology*, Vol. 14, No. 3, pp. 501–510, 2006.

[8] M. Defoort, J. Palos, A. Kokosy, T. Floquet, W. Perruquetti, and D. Boulinguez, 'Experimental motion planning and control for an autonomous nonholonomic mobile robot', *Proc. of IEEE International Conference on Robotics and Automation*, pp. 2221–2226, Roma (Italy), 2007.

[9] W.E. Dixon, D.M. Dawson, and E. Zergeroglu, 'Robust control of a mobile robot system with kinematic disturbances', *Proc. of IEEE Int. Conf. on Control Applications*, pp. 437–442, 2000.

[10] W. Dong, and W. Huo, 'Tracking control of wheeled mobile robots with unknown dynamics', *Proc. of IEEE Int. Conf. on Robotics and Aumation*, pp. 2645–2650, 1999.

[11] R. Fierro, and F. Lewis, 'Control of a nonholonomic mobile robot: backstepping kinematics into dynamics', *Journal of Robotic Systems*, Vol. 14, No. 3, pp. 149–163, 1997.

[12] M. Fliess, J. Lévine, P. Martin, and P. Rouchon, 'Flatness and defect of nonlinear systems: introductory theory and examples', *International Journal of control*, Vol. 61, No. 6, pp. 1327–1361, 1995.

[13] M. Fliess, J. Lévine, P. Martin, and P. Rouchon, 'Design of trajectory stabilizing feedback for driftless flat systems', *Proc. of the 3rd. European Control Conference*, pp. 1882–1887, 1995.

[14] M. Fliess, and C. Join, 'Intelligent PID Controllers', *Proc. of the 16th Mediterranean Conference on Control and Automation*, pp. 326–331, Ajaccio (France), 2008.

[15] M. Fliess, and C. Join, 'Commande sans modèle et commande à modèle restreint', *e-STA*, Vol. 5, 2008 (available at `http://hal.inria.fr/inria-00288107/en/`).

[16] T. Fukao, H. Nakagawa, and N. Adachi, 'Adaptive tracking control of a nonholonomic mobile robot', *IEEE Transactions on Robotics and Automation*, Vol. 16, No. 5, pp. 609–615, 2000.

[17] C.B. Low, and D. Wang, 'GPS-based tracking control for a car-like wheeld mobile robot with skidding and slipping', *IEEE/ASME Transactions on Mechatronics*, Vol. 13, No. 4, pp. 480–484, 2008.

[18] H. Martinez-Barbera, J.P. Canovas, M. Zamora, and A. Gomez, 'I-Fork: a flexible AGV system using topological and grid maps', *Proc. of the IEEE Int. Conf. on Robotics and Automation*, pp. 2147–2152, Taipei (Taiwan), 2003.

[19] F.N. Martins, W.C. Celeste, R. Carelli, M. Sarcinelli-Filho, and T.F. Bastos-Filho, 'An adaptive dynamic controller for autonomous mobile robot trajectory tracking', *Control Engineering Practice*, Vol. 16, No. 11, pp. 1354–1363, 2008.

[20] M. Mboup, C. Join and M. Fliess,'Numerical differentiation with annihilators in noisy environment', *Numerical Algorithms*, 2008.

[21] G. Genta, 'Motor Vehicle Dynamics: Modeling and Simulation', *World Scientific* , 1997.

[22] H. Nijmeijer, and W. Respondek, 'Dynamic input-output decoupling of nonlinear control systems', *IEEE Transactions on Automatic Control*, vol. 33, pp. 1065–1070, 1988.

[23] H. Pacejka, 'Tire and Vehicle Dynamics', *SAE*, 2005.

[24] P. Rouchon, M. Fliess, J. Lévine, P. Martin, 'Flatness and motion planning: the car with n trailers", *Proc. of European Control Conference*, pp. 1518–1522, Groningen (Netherland), 1993.

[25] J. Villagra, B. d'Andréa-Novel, M. Fliess, and H. Mounier, 'A diagnosis-based approach for tire/road forces and maximum friction estimation', *submitted to Control Engineering Practice*

[26] J. Villagra, B. d'Andréa-Novel, M. Fliess, and H. Mounier, 'Robust grey-box closed-loop stop-and-go control', *47th IEEE Conference on Decision and Control*, Cancun (Mexico), 2008.

[27] D. Wang, C. Boon Low, 'Modeling and Analysis of Skidding and Slipping in Wheeled Mobile Robots: Control Design Perspective', *IEEE Transactions on Robotics*, Vol. 24, No. 3, pp. 676–687, 2008.

[28] J. Wit, C. Crane, and D. Armstrong, 'Autonomous ground vehicle path tracking' *Journal of Robotic Systems*, Vol. 21. No. 8, pp. 439–449, 2004.